N.B. Volkov[*], S.V. Barakhvostov[*], A.I. Lipchak[*],
S.I. Tkachenko[**], and A.P. Yalovets[***]

PECULARITIES OF PICOSECOND RELATIVISTIC BEAMS INTERACTION WITH A METALLIC TARGET

[*] Institute of Electrophysics UB RAS
Amundsen Street 106, Yekaterinburg 620016, Russia
E-mail: nbv@iep.uran.ru
[**] Moscow Institute of Physics and Technology (State University),
Dolgoprudny, Moscow Region 141701, Russia
[***] South Ural State University, Chelyabinsk 454080, Russia

This work was performed as part of State Task No. 0389-2015-0023, and under the partial financial support of the RFBR in terms of an optical measuring of the surface velocity of the target and the results obtained with its help (project No. 16-08-00466).

OVERVIEW

- **Introduction;**
- **Experimental Setup;**
- **Interferometric measurements of target-rear-side velocity;**
- **Discussion;**
- **Conclusion**

Electron Beam interaction with different targets

Pulse of Charged Particles

Applications

- Industrial
- Material
- Medical
- *Scientific*

Imitation experiments

- short and ultra-short thermal impact
- *shock and acoustic waves in solids*
- EM radiation *(λ = 10 nm ÷ 10^{-2} m)*
  - *electronic components & construction materials for nuclear fusion reactors & spacecraft applications*

High-Energy Densities and Fundamental Physics

- particles beams generation
- intense radiation initiation
- beam-matter interactions

The generators, allowing to acquire high-voltage pulses with voltage amplitude $U_{max} \approx 200$ ***kV***, duration $\tau_p \leq 1$ ***ns*** and voltage rise rate ***dU/dt ≥ 1 MV/ns*** are of great interest for studying of *fast non-linear electrodynamic process in quantum plasma investigation*.
At that one can limit to the value of the stored energy at the level of about ***W = 1-10 J***

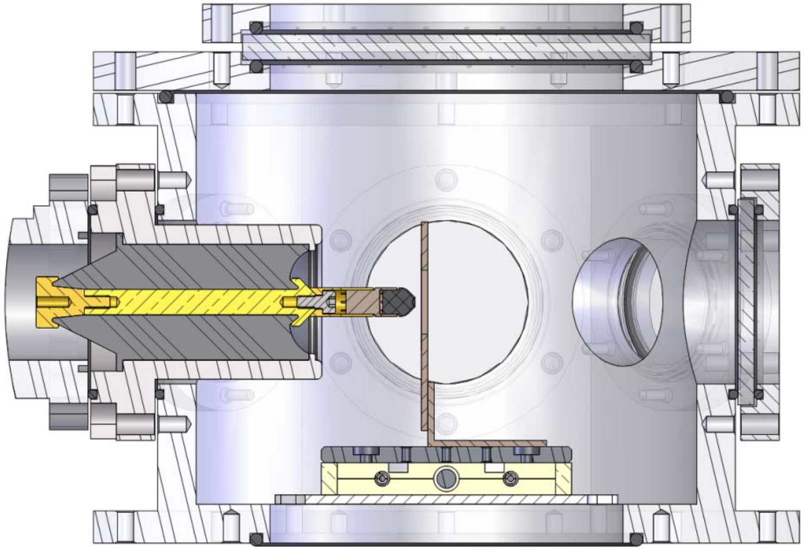

Experimental Setup

«RADAN-300» series HVPG

voltage pulse refined and shortened to amplitude of about 150 kV and duration < 600 ps (front < 300 ps fall < 200 ps)

Target (anode):
Two Cu foils 18μm thickness
Cathode:
Sm, Cu, W and Graphite rods with cone in 2 mm diameter

Remote controlled Vacuum Pumping System

EMP-shielded measurements chamber

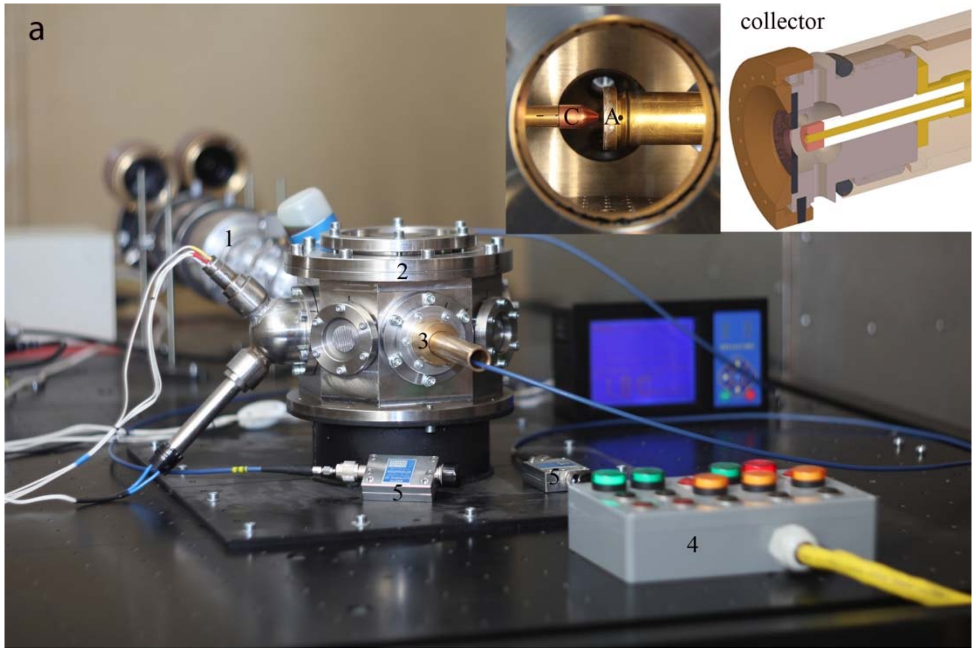

Measuring Equipment

Oscilloscope

Tektronix

mod. DPO70404C

4-channel, 4 GHz bandwidth
analog sample rate 25GS/s

HUBER+SUHNER
Excellence in Connectivity Solutions

Sucoflex 18 GHz coaxial cable assembies

Attenuators

Barth Electronics, Inc.

mod. 142-NMFP-20B

high-voltage pulse rated for 2.5 kV / 400 ns
50 Ω impedance *20 dB attenuation*
unique precise voltage ratio factory measured
up to 30 GHz bandwidth

AEROFLEX
WEINSCHEL

mod. 23-6-34 and mod. 23-20-34

6 dB attenuation 20 dB
50 Ω impedance
peak power rated for 1 kW / 1μs
up to 18 GHz bandwidth

Beveled-head current collector cross-section

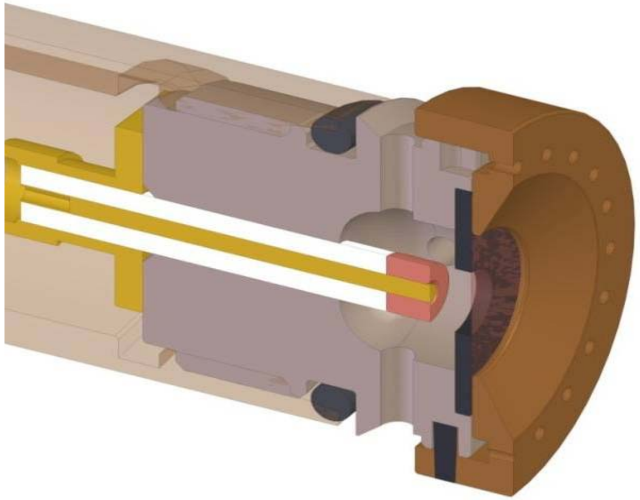

2mm inter-electrode gap, Cu cathode

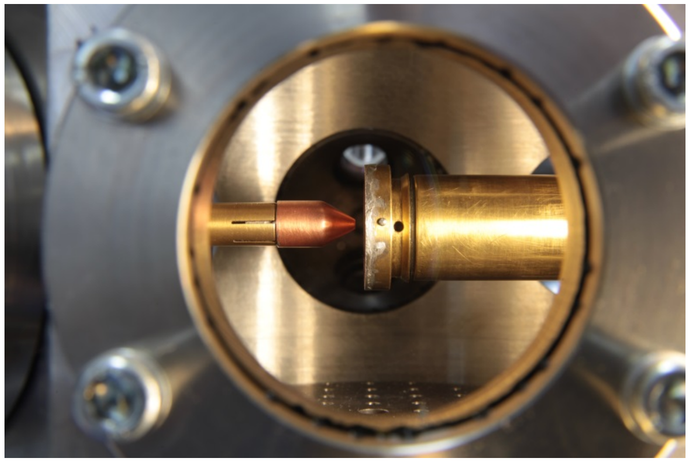

Typical oscillograms of voltage (Ch1) on an entrance of the coordinating oil line 30 cm long and a beam current (Ch2) on the collector after passing two copper foils 18 microns thickness.

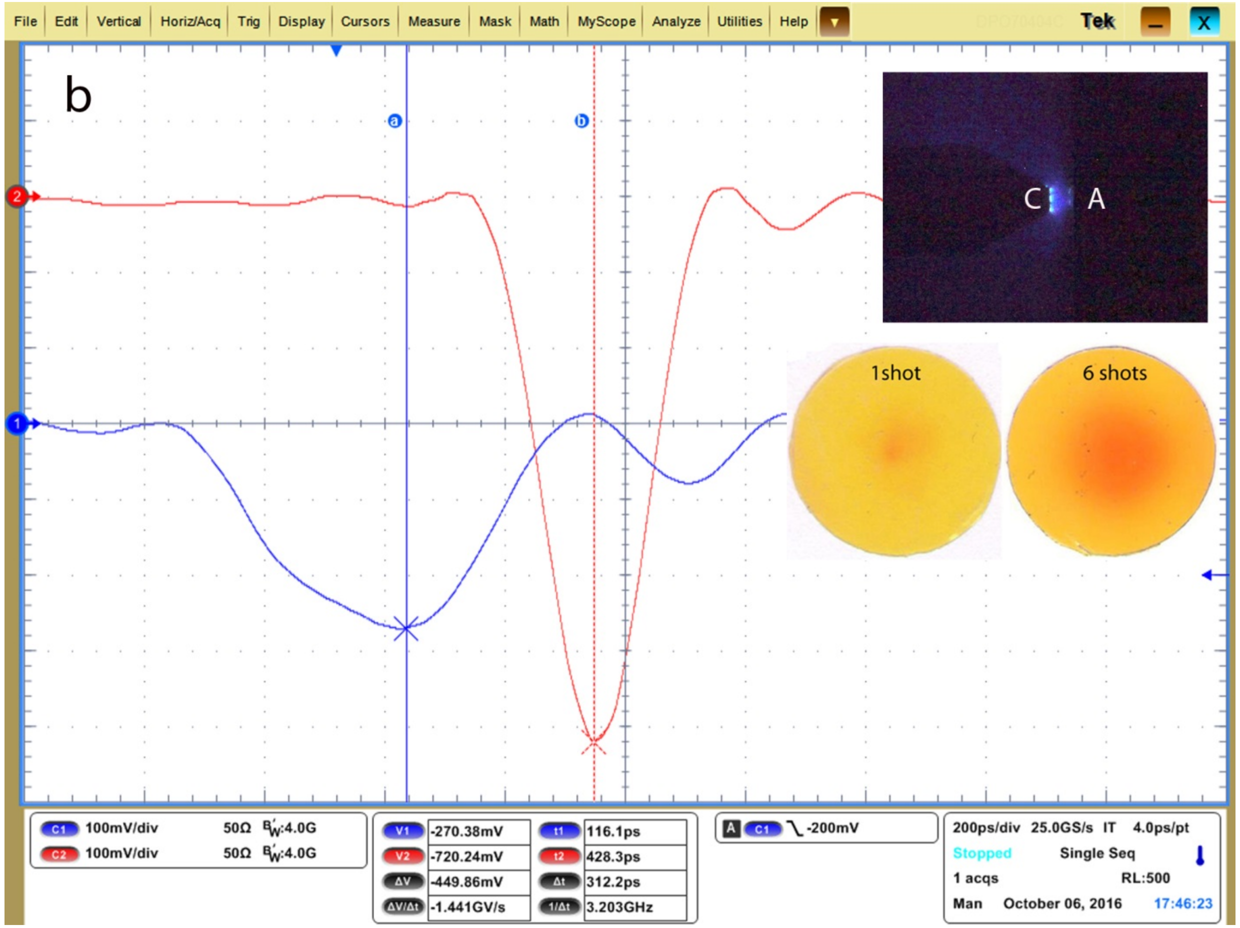

Intensity of the electron beam image on dosimetric film has view:

For 6 shots – XZ (left) and YZ (right) cross-sections; for one shot.

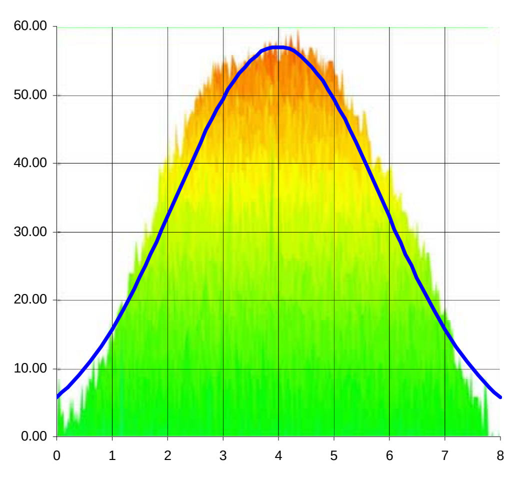

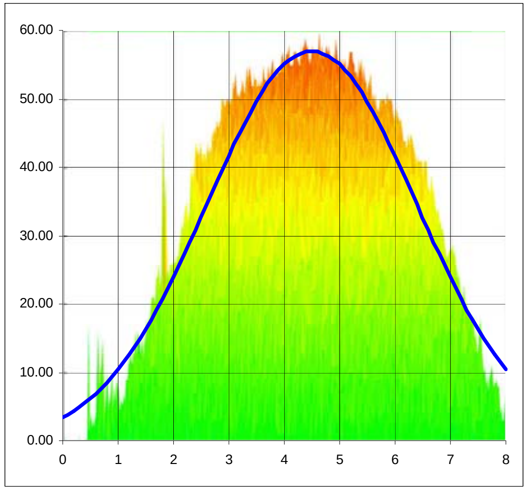

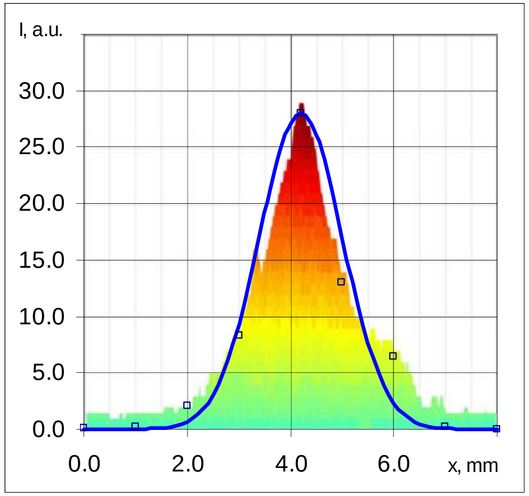

It is described by the Gauss formula $I(x) = \frac{A}{\sqrt{2\pi}} \exp\left(-\frac{(x-x_0)^2}{2\sigma^2}\right)$, where:

Cross-section	A	x_0, mm	σ, mm	FWHM*, mm
XZ	22.74	4.0	1.87	4.41
YZ	22.74	4.5	1.89	4.43

A	x_0, mm	σ, mm	FWHM, mm
11.17	4.2	0.81	1.90

* FWHM is the full width on a half amplitude level.

Interferometric measurements of target-back-side velocity

a

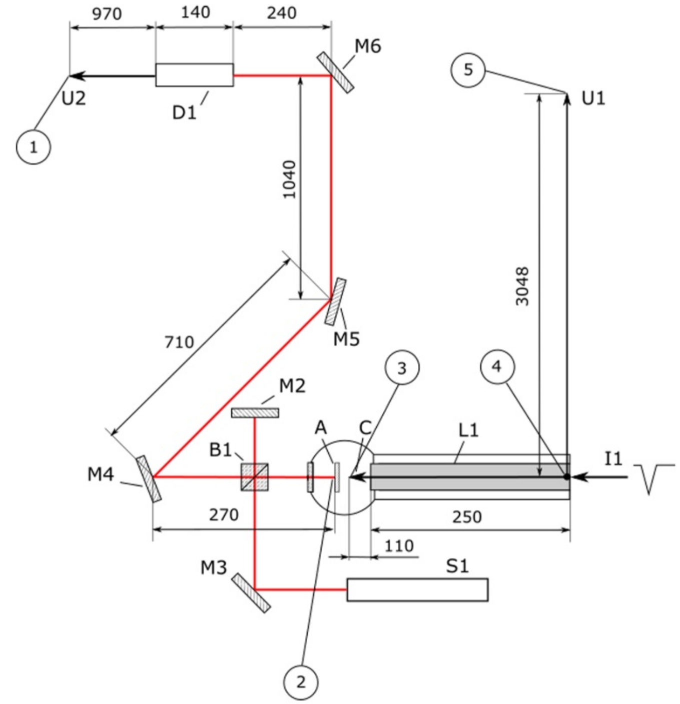

b

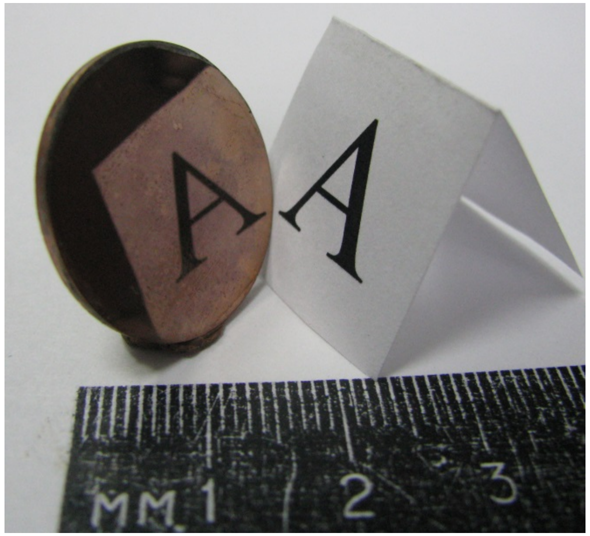

c

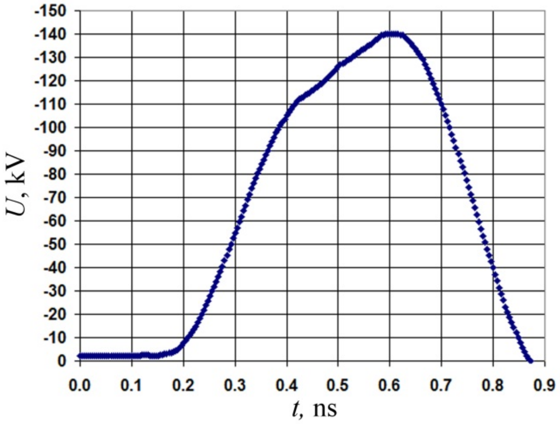

a) The scheme of the interferometer. The figure shows the dimensions in mm for delays calculating. 1 is the "U2" input of the oscilloscope, 2 is the anode, 3 is the cathode, 4 is the voltage divider, 5 is the "U1" input of the oscilloscope; b) rear side of the anode which is mirror of the interferometer; c) electron beam voltage waveform.

a **b**

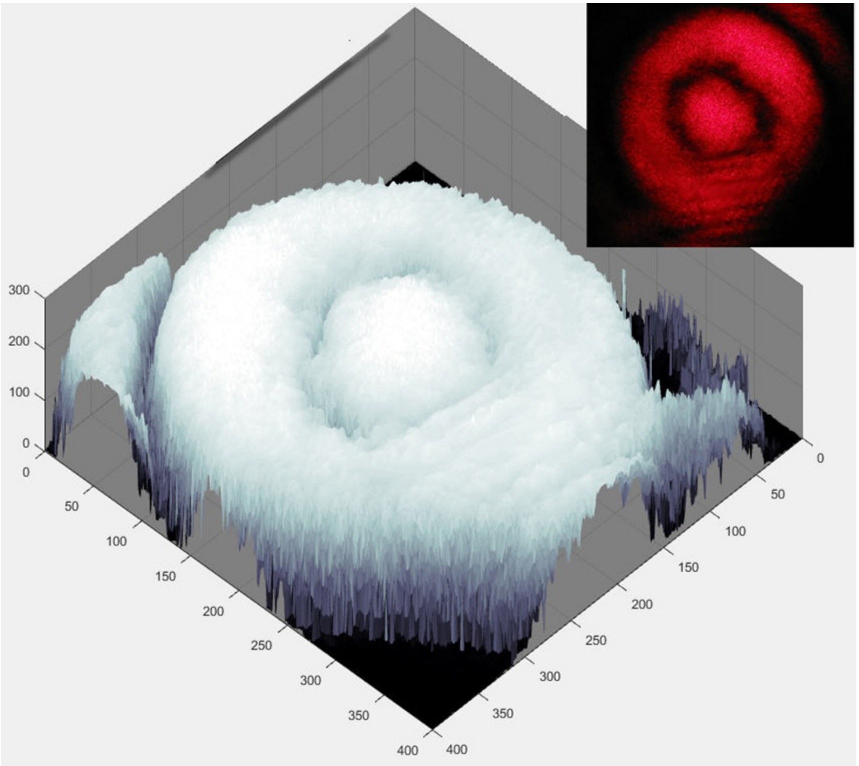

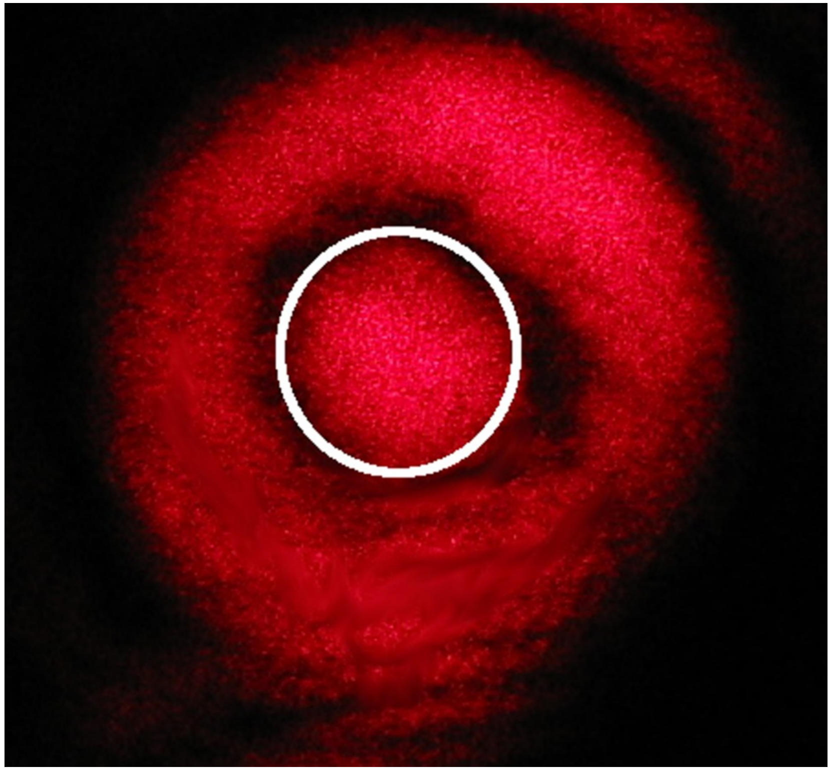

a) Interference image and the intensity profile; b) the central fringe of the interference image (marked by the white circle).

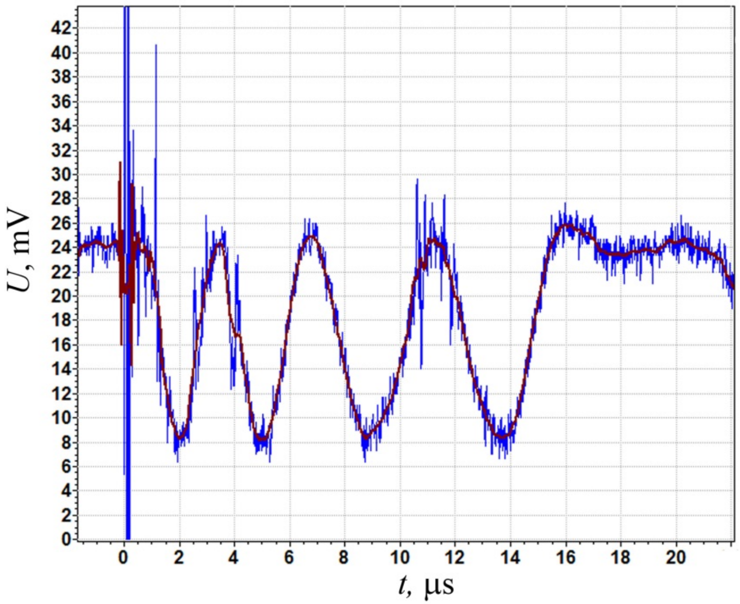

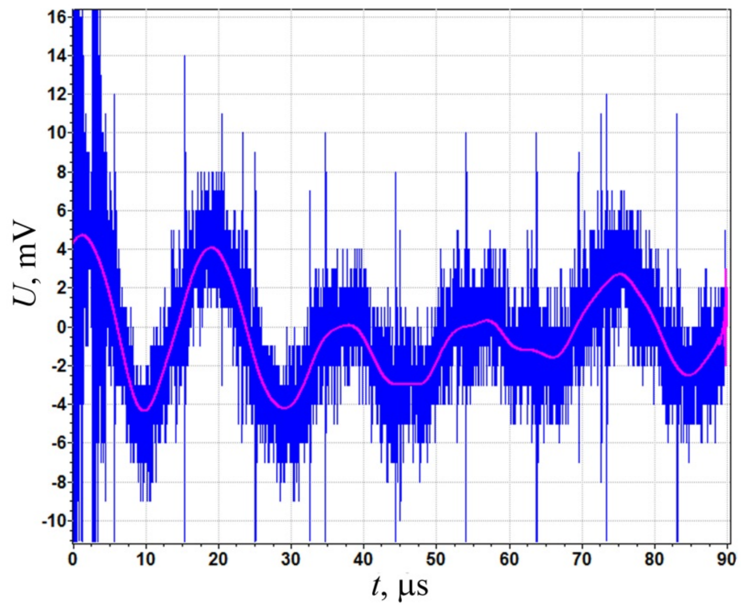

The typical photodiode (D1, Fig. 2a) signals at different anode thickness: the left image shows results for the 0.1 mm and the right - 3mm).

It is common knowledge the interference signal is described by the following equation

$$I = I_0 + I_s \cos\left(\frac{2\pi\Delta}{\lambda}\right),$$

where I_0, I are the amplitudes of constant and variable components, respectively, Δ is the optical path difference, λ is the laser wave length (in our case λ = 632.8 nm). The difference in arms length of the interferometer is $x = \Delta / 2$. For example, if the "A" mirror shift is $\lambda / 2$ (i.e. length difference of interferometer arms change), then the optical path difference will be changed on λ and the phase difference change will be 4π .

Then coordinate of the target-back-side and amplitude of the interferometric signal intensity are

$$x(t) = x_0 + x_1 \sin\left(\frac{\pi(t-t_0)}{T}\right) \Rightarrow I = I_0 + I_s \cos\left(\frac{4\pi}{\lambda}\left(x_0 + x_1 \sin\left(\frac{\pi(t-t_0)}{T}\right)\right)\right),$$

where x_0 is the initial optical path difference, t_0 is the delay time of the displacement beginning of the anode rear surface relatively electron beam action, x_1 is displacement amplitude, T is displacement period.

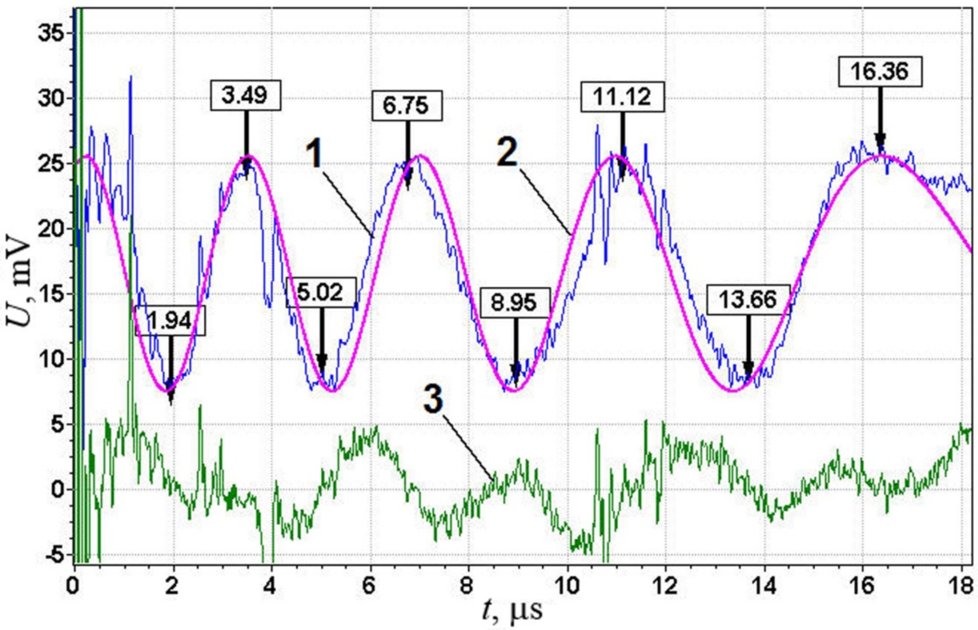

Example of the approximation of the photodiode signal for target thickness 0.1 mm: 1) experimental data; 2) approximation results for parameters $x_0 = -1.30 \cdot 10^5$ nm, $x_1 = 1.32 \cdot 10^5$ nm, $t_0 = -259.06$ ns, $T = 575.11$ns; 3) difference between the experimental and approximation data.

Results of interferometric measurements

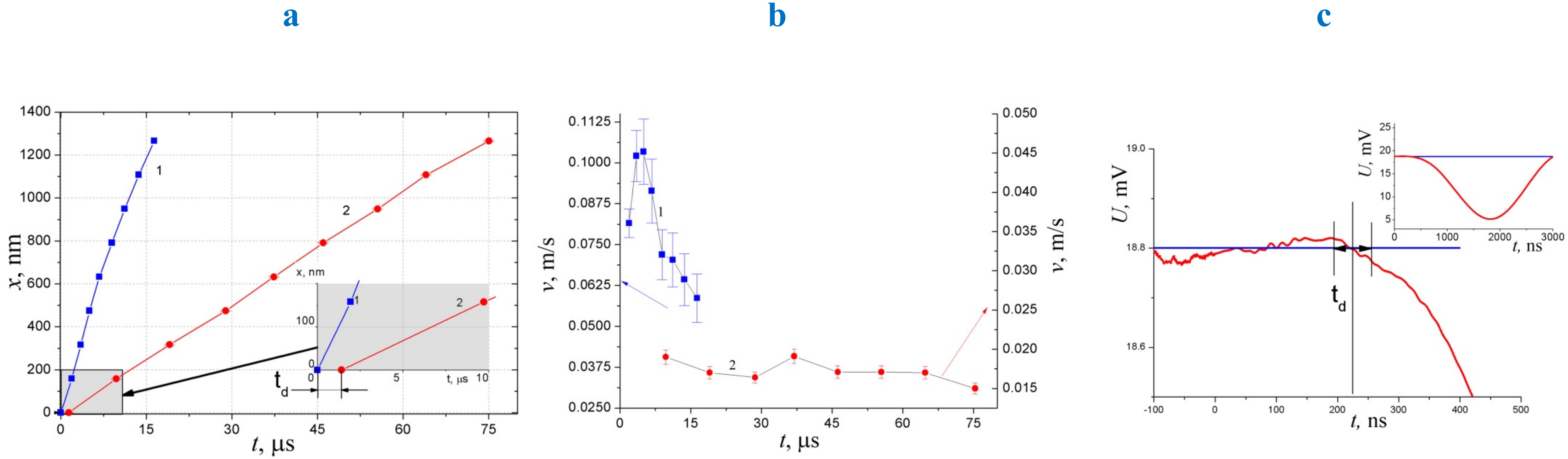

The time dependencies of the displacement (a) and velocity (b) of the central part of the rear side of the anode with the thickness of 1) 0.1 mm, 2) 3 mm. The waveform (c) of the photodiode signal for the anode thickness of 0.1 mm shows displacement delay time t_d and its accuracy (the displacement of the anode rear side with thickness of 0.1 mm is stably recorded with delay of t_d= 225±30 ns being in a good agreement with the parameter of -t_0= 259.06 ns in relations x(t) and I(t) for an anode thickness of 0.1 mm.).

DISCUSSION

I. Several estimates of surface forces: A magnetic pressure.

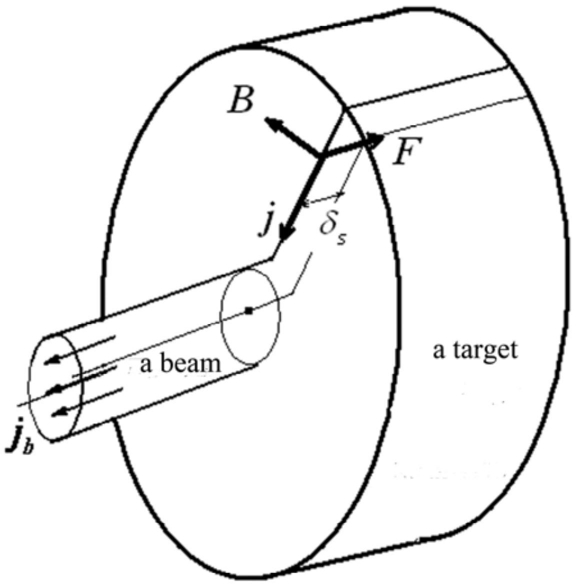

Qualitative picture of the beam current interaction with the current induced by the beam in the target.

Based on the figure, the following estimate of the magnetic pressure acting on the target surface can be obtained:

$$P_b(r) = \begin{cases} \dfrac{\mu_0 I_b^2}{8\pi^2} \dfrac{r^2}{r_b^4}, r \le r_b \\ \dfrac{\mu_0 I_b^2}{8\pi^2 r^2}, r > r, \end{cases}$$

Where I_b, r_b **are the current and the radius of the beam respectively. The pressure maximum corresponds to the equality** $r = r_b$ **:**

$$P_{b,\max} = P_b(r_b) = \begin{cases} \dfrac{\mu_0 I_b^2}{8\pi^2 r_b^2}. \end{cases}$$

The experimental values of the current, 200 A, and the beam radius, 2 mm, correspond to a pressure value less than 1 kPa. ***This pressure acts within 0.5 ns and can not provide the observed in the experiment, the displacement of the surface of the target.***

II. An electrical pressure.

Suppose that, due to the short duration of irradiation, electrons of the beam accumulate near the target surface. Assuming in the first approximation that the absorbed-beam-electrons charge is the surface charge, it is possible to obtain an upper estimate of the pressure on the target resulting of the charge interaction with the diode's electric field:

$$P_b(r,t) = E_z \cdot q_{surf}(r,t) = E_z f(r) \int_0^t I_b(t')dt'.$$

Numerical estimates show that to achieve the experimental velocity value of ~ 0.1 m/s of the target with a thickness of 100 μm at a beam energy of 12.65 mJ), a field with a strength of more than 100 MV/cm is required. The experimental values of the target displacement cannot be achieved due to large energy losses due to plastic deformation, since the maximum pressure in the center of the target at the end of irradiation reaches 1 GPA.

Conclusion: ***It is impossible to explain the experimental values of the displacement and velocity of the rear side of the target by the surface interaction of the beam and target currents and the charge of absorbed electrons in the target with the electric field of the diode!!!***

Some remarks about simulation of these experiments

The simulation was carried out within the framework of software realizing the solution of the equations of two-dimensional axisymmetric single-temperature mechanics of a continuous elastoplastic medium [Leyvi A.Y. and Yalovets A.P 2016 *Simulation of Power Plasma Flows Impact on Matter* (Chelyabinsk: City-Print)]. The purpose of this simulation was to evaluate the wave processes role occurring inside the anode caused by the action of the electron beam of 500 ns duration and the space-time evolution of the thermodynamic and mechanical anode matter characteristics. **The system of the equations includes equations for the energy release calculation function in a matter irradiated by the beam; movement and energy balance equations; wide-range state equation and also equations for the stress tensor of a continuous medium. Calculation of the energy release function in matter under the fast electrons beam action is based on the solution of the corresponding kinetic equations. To solve the equations system for the continuum mechanics the numerical-analytic method proposed in [Yalovets A P 1997 *J. Appl. Mech. Tech. Physics* No 1 151] was used. Since the duration of the electron beam irradiation in our experiments was only 0.5 ns, we used the simplest Mie–Gruneisen state equation. The calculated area had a radius of 3.5 mm. The target thicknesses were equal to 0.1 and 3 mm in the calculations. The total beam energy was 0. 01256 and 0.1256 J. The current density distribution was determined in the Gaussian form with a dispersion parameter of mm according to prints on the radiochromic film of the electron beam.**

The numerical results show the temperature of the anode material increases only for few degrees in comparison with the initial temperature (300 K). At the same time, the mechanical stresses reached tens MPa, but not reaching of 68.5 MPa yield strength point for copper. The calculated displacement of the anode rear side with a thickness of 3 mm did not exceed 10 nm, which is 2 orders of magnitude less than the one observed in the experiment. In our opinion, this is due to ignoring of the interaction peculiarities of the electron beam with duration less than 1 ns with the target. The main of these peculiarities is defined by fact that during the irradiation the beam charge introduced into the anode with almost motionless ions induces in it electric (electronic) currents. The interaction of these currents with the beam main current leads to a much more intense mechanical action on the anode matter.

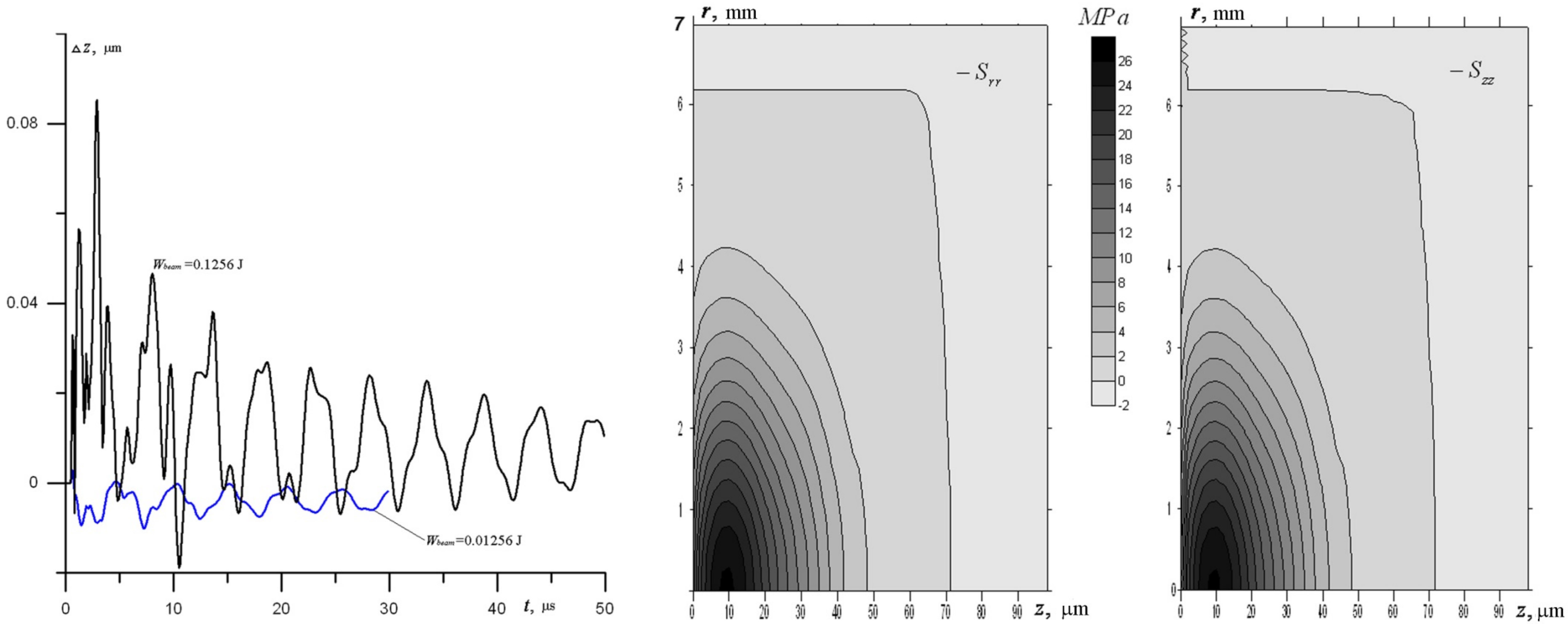

<u>Left:</u> The displacement of the anode read side with thickness of 0.3 mm; <u>Right:</u> The space distribution of the stress tensor components in the copper anode with thickness of 0.1 mm.

<u>Problem:</u> ***It is impossible to explain the features of the interaction of a picosecond relativistic electron beam with a metal target observed in our experiments without taking into account the effect on the quasi-neutral in the initial state of the metal ion-electronic system of the absorbed- beam-electrons charge!!!***

Our work aimed at solving the formulated problem.

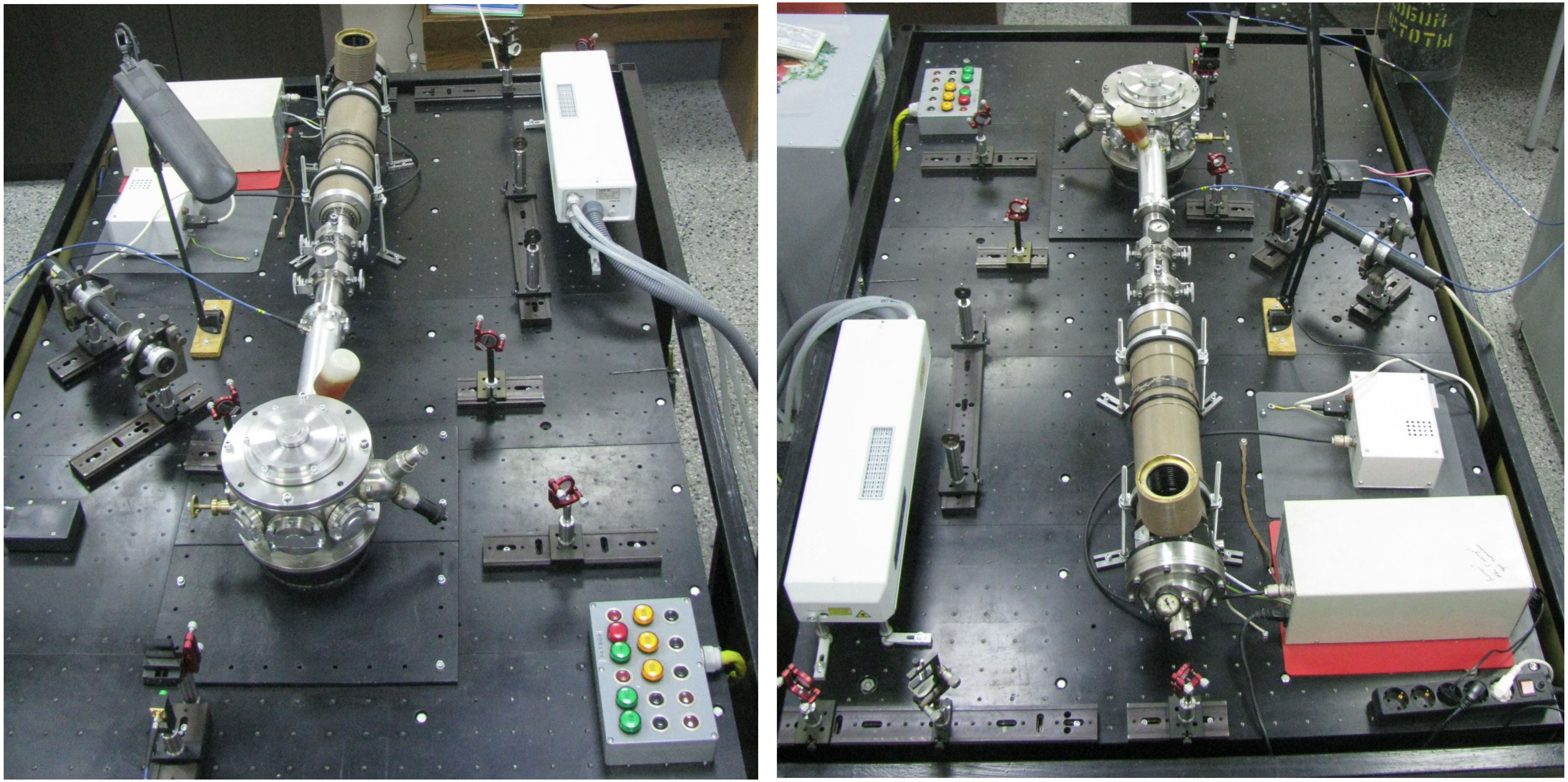

Appearance of the EXCITOR experimental setup from the side of the vacuum chamber (left) and from the side of the discharger (right).

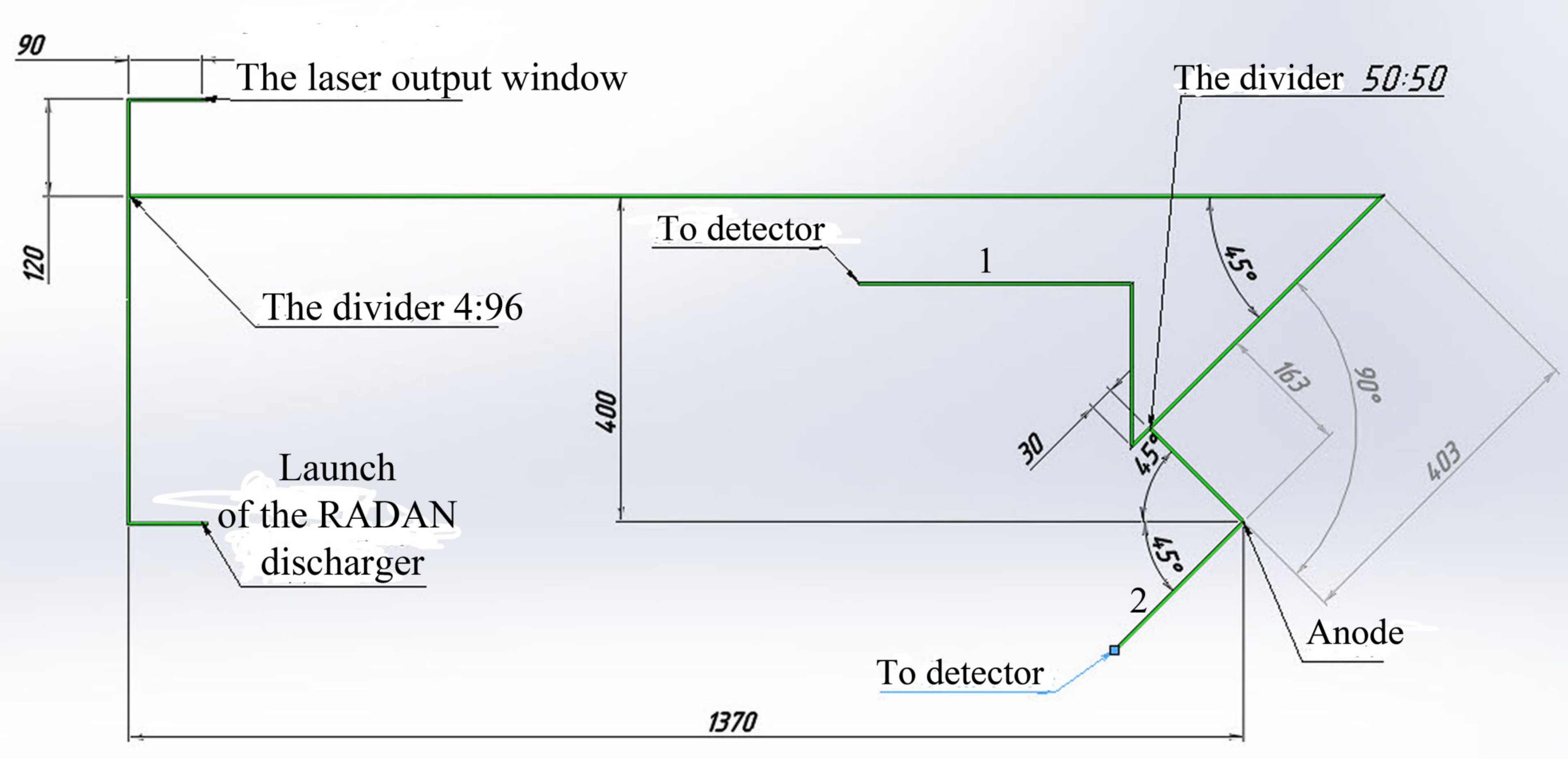

Optical scheme for registration of the module of the absorption coefficient of laser radiation in a metal excited by a picosecond electron beam and ignition of the triggering discharger of the RADAN generator.

The triggering discharger of the RADAN generator

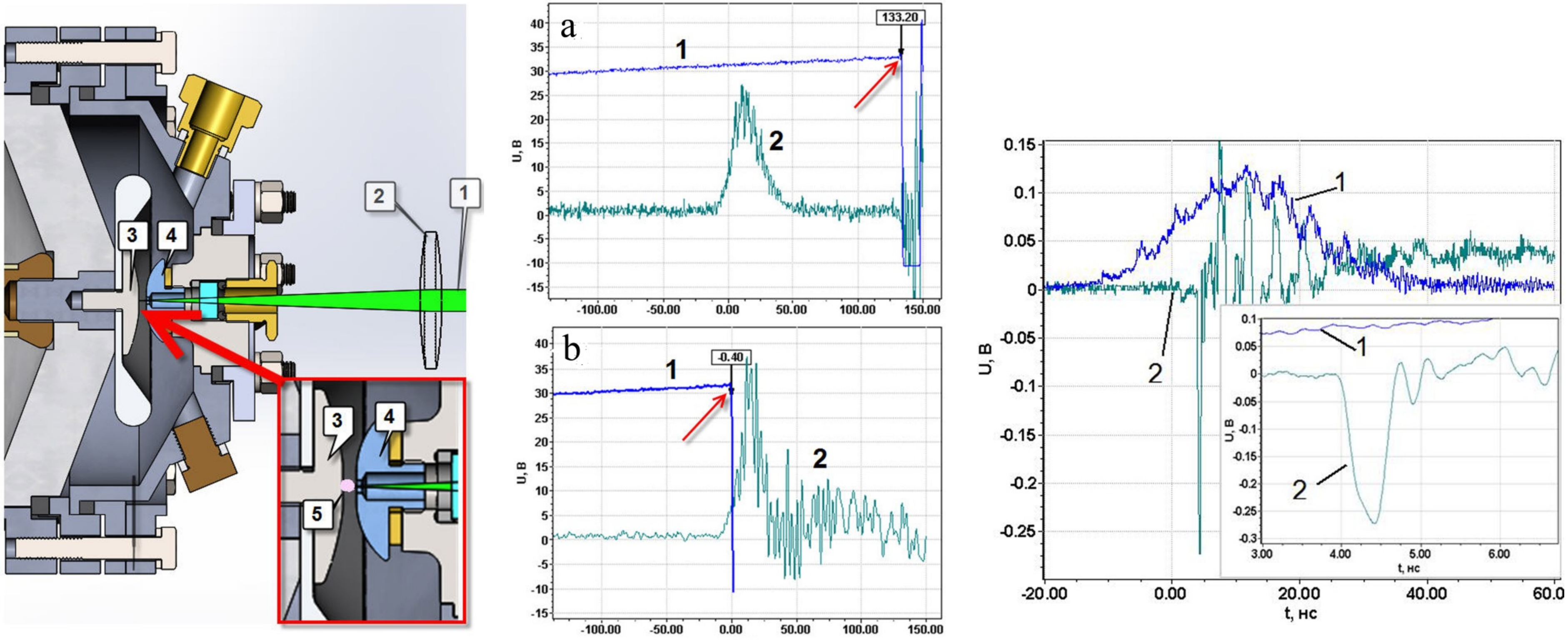

a b c

a) 1 – A laser radiation; 2 – a focusing lens; 3 – an anode; 4 – a cathode; b) 1 – the voltage n the secondary winding of the Tesla transformer of the RADAN generator (in the upper figure, the discharger window is closed for laser radiation); 2 – the laser radiation; c) 1 - the laser radiation; 2 – the voltage pulse at the output of the slicer. *Currently, the jitter of the spark gap ignited by the laser radiation is 1.76 ns.*

Conclusions

Thus, in our work:

1. An interferometric technique of recording of the anode rear side displacement as a result of the irradiation by the picosecond electron beam was implemented.
2. It is impossible to explain the experimental values of the displacement and velocity of the rear side of the target by the surface interaction of the beam and target currents and the charge embedded in the target with the electric field of the diode.
3. In case of the appropriate modification of the theoretical model this technique will allow one within the framework of the continuum mechanics to investigate the slow spatiotemporal evolution of the non-equilibrium states of a metal excited by such irradiation.
4. The results of experiments on the creation of a launching discharger with the ignition of laser radiation are discussed. It is established that the jitter of the discharger amounted to 1.76 ns.

Many thanks for Your kind attention!!!